Turkish Journal of Electrical Engineering & Computer Sciences

http://journals.tubitak.gov.tr/elektrik/

Research Article

Turk J Elec Eng & Comp Sci
(2019) 27: 2295 – 2308

doi:10.3906/elk-1804-45

An analytical formula for selecting the feeding voltage and frequency in a TORUS-type nonslotted axial flux permanent magnet machine design

Reza MIRZAHOSSEINI*, **Ahmad DARABI**, **Mohsen ASSILI**
Department of Electrical and Robotic Engineering, Faculty of Electrical Engineering and Robotics, Shahrood University of Technology, Shahrood, Iran

Received: 06.04.2018 • **Accepted/Published Online:** 06.01.2019 • **Final Version:** 15.05.2019

Abstract: Axial flux permanent magnet (AFPM) motors are usually controlled by drive; therefore, in the design of these machines the feeding voltage and frequency are completely independent parameters. Undoubtedly, the values of these parameters have significant effects on the performance characteristics of the machine. The main objective of this paper is to investigate the effects of these parameters on the efficiency of a double-sided TORUS-type nonslotted (TORUS NS) AFPM motor and propose a formula for selecting the optimal values of the feeding voltage and frequency at the beginning of the design process. To fulfill this goal, different machines with various speeds, powers, and feeding voltages are designed based on a proposed design algorithm. Then a formula for calculating machine efficiency is presented based on the frequency, number of pole pairs, output power, and feeding voltage of the machine. In order to confirm the validity of the proposed formula, several fabricated machines with different powers and speeds are selected as case studies. The efficiency of these machines is calculated using the proposed formula and is measured in the laboratory. Comparing the results confirms the excellent accuracy of the proposed formula.

Key words: TORUS-type nonslotted axial flux permanent magnet (TORUS NS-AFPM) machine, design algorithm, performance characteristics, feeding voltage, optimum frequency

1. Introduction

The history of electrical machines shows that the first axial flux machine was introduced by Faraday in 1821 [1]. However, axial flux structures have been discarded for several years because of high price of permanent magnet materials, difficulty of balancing, difficult axial lamination of slotted stator core, and assembly problems. With the development of permanent magnet materials and power electronic devices, the axial flux permanent magnet (AFPM) machine has attracted more attention due to its high torque density, high efficiency, high diameter-to-length ratio (compactness), and low noise level [2–8]. The torque density of small size axial flux motors is twice as high as its radial flux counterpart [9]. Today AFPM motors are employed in direct-drive traction applications due to their wide speed range operation capacity [10]. Several topologies have been proposed for AFPM machines, which can be classified into three major categories: 1) single-sided AFPM machines, 2) double-sided AFPM machines, 3) multistage (multidisc) AFPM machines. The stator of these topologies can be slotted or nonslotted [11–16]. The rotor structure can have surface-mounted or interior-mounted magnets [17]. The nonslotted axial flux topologies have higher torque density, higher efficiency, better heat scattering, and lower noise level than the slotted axial flux topologies [18–20]. In the nonslotted machine, the effective air

*Correspondence: reza.mirzahosseini78@gmail.com

gap is inevitably very large, which results in limiting the flux density variations due to the magnetomotive force (MMF) harmonic components and thus the rotor iron losses [21]. In addition, the nonslotted topologies usually have ignorable cogging torques and consequently the minimum level of torque ripples and lower sound level. Especially, the TORUS NS topology has the minimum sound power level amongst all the different topologies [18–20]. In addition, the double-sided AFPM machine with dual rotor produces more torque than a single-sided structure with in a limited space [22]. According to all performed investigations as well as the above considerations, the TORUS NS-AFPM motor with a nonslotted stator in the middle and two disc type rotors at the sides is selected here as the best topology for consideration. Several works have already been accomplished about the design, optimization, and performance improvement of the TORUS NS-AFPM motor. Gieras et al. published a book about the different aspects of AFPM machines, such as various structures, sizing equations, materials, fabrication, industrial applications, control, cooling, and heat transfer [11]. Huang et al. compared various types of PM motors, such as slotted and nonslotted radial flux permanent magnet (RFPM) and AFPM, from the viewpoints of power density, heat transfer, torque ripple, and acoustic noise generation [18]. Also, Huang et al. presented the sizing equations for two major types of double-sided AFPM motors, i.e. two-rotor one-stator and two-stator one-rotor structures, and then compared the power densities and efficiencies of the two structures [23]. Mahmoudi et al. compared the TORUS and axial flux interior rotor (AFIR) structures from the viewpoints of power density and torque quality. Also, they presented the sizing equations of these structures [24]. They showed that TORUS topology has high power density in high current density and low electrical loading. Baghayipour et al. proposed an analytical method for calculating the harmonic content of back EMF in a TORUS NS-AFPM machine considering the winding distribution and iron saturation effects. They validated the proposed method with the help of the finite element method (FEM) and by measurement in the laboratory [25]. Although several references have been published in the field of design and performance improvement of the TORUS NS-AFPM machine, our investigations show that no analytical formula has been presented to choose the frequency, number of pole pairs and feeding voltage regarding the performance characteristics of the TORUS NS-AFPM machine. Therefore, the main objective of this paper is to investigate the effect of these three parameters on the performance characteristics of the TORUS NS-AFPM machine and present an analytical formula for optimal selection of them at the beginning of the design process. For this purpose, first, the structure of the TORUS NS-AFPM machine is introduced and its operation is described in detail. Then, with the help of the sizing equations presented in the previous references, an algorithm is suggested to study the effect of the frequency, number of pole pairs, and supply voltage on the performance characteristics of the TORUS NS-AFPM machine. By using the proposed algorithm, several motors are designed and the effect of frequency, number of pole pairs, power supply voltage, and motor output power on the efficiency of the motors are investigated. Finally, a formula for calculating efficiency in terms of these four parameters is presented.

2. TORUS NS-AFPM structure

The structure of the TORUS NS-AFPM is illustrated in Figure 1 [18]. According to Figure 1, the motor has a stator that is located between two rotor discs. The stator core is manufactured from the spiral laminated silicon–iron sheet and a three-phase winding with back-to-back connection is warped around it. The rotor comprises two magnetic discs and a few permanent magnets so that permanent magnets are placed in the inner surface of the magnetic discs. The structure of the motor involves a number of pole pairs lied beside each other along the periphery. One pole pair structure is depicted in Figure 2. The magnetic flux paths inside the motor is shown in this figure. It is noted that the armature current and permanent magnets generate magnetic flux

in the air gap. However, most part of the flux is due to permanent magnets [26]. According to Figure 2, the magnetic fluxes of permanent magnets pass through the air gap and then enter into the stator core. These fluxes after passing the stator core enter into the air gap and then two adjacent permanent magnets.

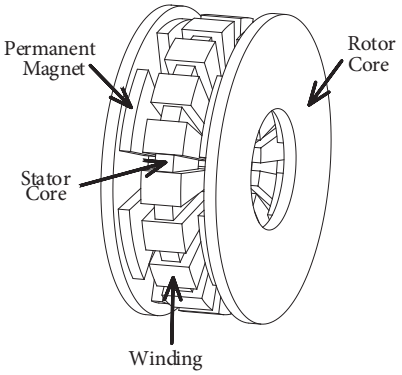

Figure 1. The structure of TORUS NS-AFPM motor.

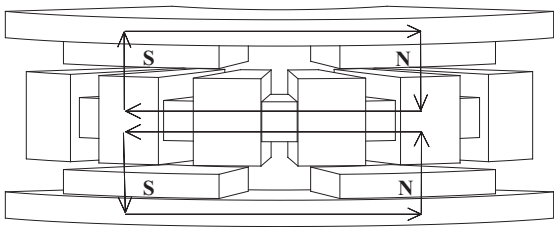

Figure 2. One pole pair of TORUS NS-AFPM motor.

3. The effect of frequency on the machine performance

At the initial step of designing a machine, the output power, nominal speed, and the minimum acceptable efficiency are usually specified. For designing a machine at a specified speed, the ratio of the frequency to the number of pole pairs is constant. In other words, by increasing (decreasing) the frequency, the number of pole pairs also increases (decreases). Therefore, the changes in these two factors must be considered together. The change in frequency and consequently the number of pole pairs affect the dimensions and performance characteristics of the machine, such as the efficiency and flux density of different parts. In order to investigate the effect of frequency on the performance characteristics of the machine, an algorithm is proposed, which is shown in Figure 3. In this algorithm, the design parameters of the machine are divided into four categories i.e. machine-rated parameters, design constraints, selective design parameters and calculable design parameters. The machine-rated parameters including rated power and nominal speed are determined at the initial step of the design process. In addition, the design constraints, such as dimensional constrains (i.e. maximum outer diameter and maximum axial length of machine), minimum efficiency, and maximum weight are defined at the preliminary step of the design process. Since the number of machine design equations is less than the number of unknown variables, the designers have to select some of the values of design parameters independent from the others. These parameters are considered as selective parameters. Based on this assumption, the number of phases, winding factor, and armature current density, etc. are selective parameters. The values of selective parameters are usually selected based on experience, previous knowledge, and fabrication constraints. In addition, these parameters can be determined using optimization techniques. The calculable parameters are the parameters whose values are determined as some functions of the selective parameters via using mathematical equations. Here, the power factor, efficiency, leakage flux factor, number of turns of armature winding, machine inner and outer diameters, axial length of stator core, axial length of rotor core, axial length of PM, etc. are considered as calculable parameters. According to this category, the design algorithm depicted in Figure 3 has been proposed. At the initial step of this algorithm, the machine-rated parameters and design constraints are determined. In the next step, the values of selective parameters are determined. Then some initial values are considered for recalculable parameters (i.e. efficiency, power factor, and leakage flux factor). The values

of calculable parameters are calculated with the help of available mathematical equations and the estimated values. In the next step, the values of recalculable parameters are calculated and compared with the estimated initial values. If the error is greater than a special value, the estimated initial values are substituted by the calculated values. This process repeats until the convergence criterion is met. Then the results of the designed machine are saved. In the next step, the frequency value is increased by a specified step frequency and the design process is repeated. Here, the value of step frequency is considered to be 5. The step frequency value is an optional parameter that is determined by the designer. The design process is repeated between the frequency range of 5- f_{max}.

Based on the proposed algorithm and using sizing equations presented in [27], a sample machine with specifications given in Table 1 is designed for different frequencies. Here, the machine is designed for frequencies ranging from 5 to 200 Hz. Also, in order to create the same conditions, the amount of some design parameters, such as the ratio of the pole arc to pole pitch, the ratio of the inner diameter to the outer diameter of the machine, the terminal voltage, the back EMF and the air gap flux density, etc. in all frequencies are considered constant. Since the effective air gap of the nonslotted machine is unavoidably too big, the synchronous reactance will be very small compared to the conventional synchronous machines. It is noted that the large space occupied by the windings itself has to be considered to be a part of the effective air gap. Therefore, if the machine is designed properly, the value of the back EMF will be much closer to the terminal voltage value and the machine will operate with great stability and stiffness torque at small power angle. Otherwise, if the machine is designed with a big difference between the terminal voltage and back EMF values, the reactive lead or lag current will be so heavy that it will reduce the efficiency of the machine. In this regard, the value of back EMF can be assumed almost known previously according to the terminal voltage value. Similar discussion can yield to a constant virtually known air gap flux density. Fractional pitch winding is usually used in AC machine to reduce the harmonic contents of the air gap flux density. However, due to the inherent large effective air gap length of the TORUS NS-AFPM machine, short-chorded winding has minor effect on the harmonics of the air gap flux density. Therefore, the winding pattern is implemented simply as a full-pitch winding to avoid any reduce in the amplitude of the first harmonic of the air gap flux density. The leakage flux coefficient for various frequencies is shown in Figure 4. According to this figure, the leakage flux coefficient decreases (the leakage flux increases) by increasing frequency. In fact, since the machine speed is constant, the number of pole pairs increases by increasing the frequency, which results in increasing the leakage flux between adjacent poles. As the leakage flux increases, the air gap flux density decreases. Therefore, the height of the permanent magnet must be increased to achieve the desired flux density. In Figure 5, the variation of permanent magnet height versus frequency is shown. The variation of the machine power density versus frequency is shown in Figure 6. As the frequency increases, the machine power density increases. However, with excessive increase in frequency, the machine power density decreases due to the increase in permanent magnet height. The variation of machine efficiency versus frequency is depicted in Figure 7. According to this figure, the machine efficiency increases with an increase in frequency up to about 70 Hz. After that, further increasing the frequency decreases the machine efficiency.

4. The proposed formula for calculating machine efficiency

According to the figures, it can be concluded that the frequency has a significant effect on the performance characteristics of the machine. Since the TORUS NS-AFPM motor is controlled by the drive system, in addition to the frequency, the feeding voltage is also an optional parameter in a specified range. However,

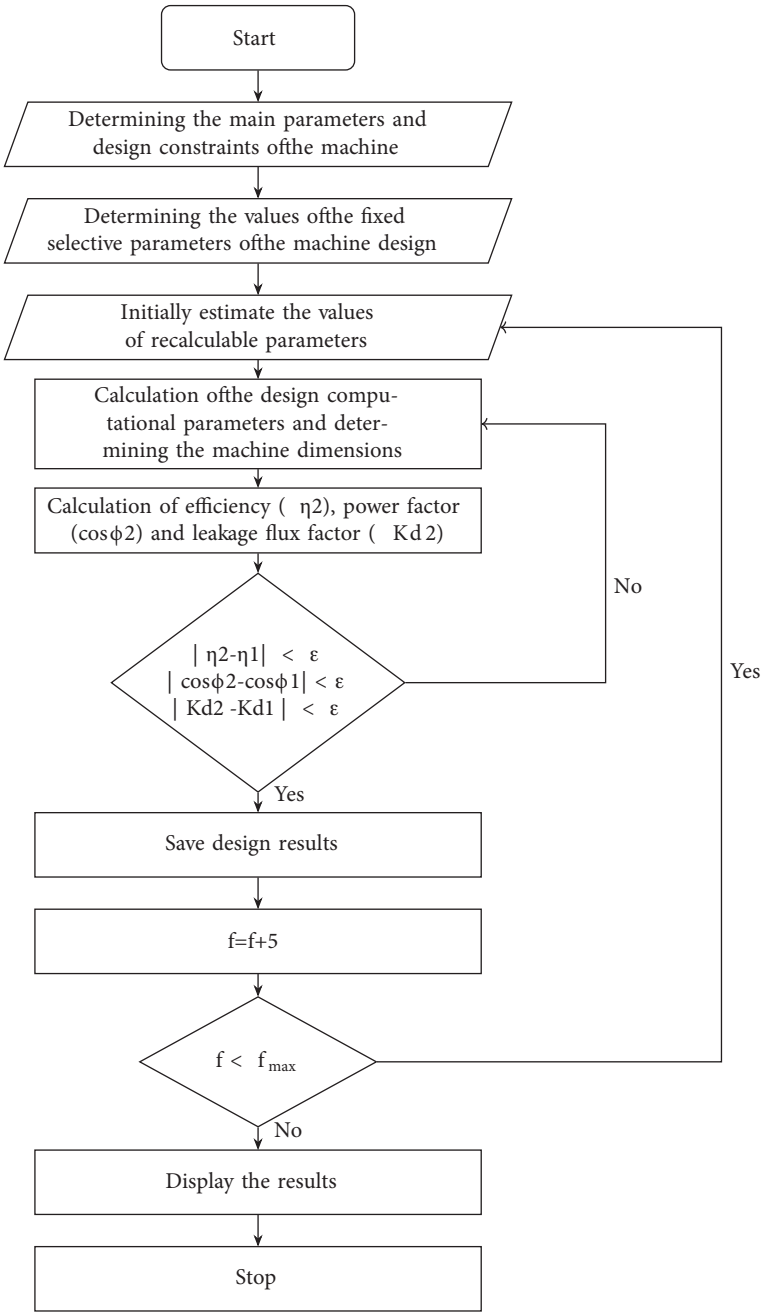

Figure 3. The proposed algorithm to perform the intended frequency studies.

our investigations show that no formula has been presented so far for selecting these optional parameters at the beginning of the design process of the TORUS NS-AFPM machine. This makes the machine designer confused in choosing the values of these parameters. The machine efficiency is one of the most important performance characteristic in the design of any electrical machine. In addition to optional parameters, the output power and speed of the machine also affect the machine efficiency. The machine speed depends on the frequency and the number of pole pairs. Therefore, in order to obtain a formula for determining efficiency at the beginning of design process, the effect of changes in the four parameters of feeding voltage, output power, frequency,

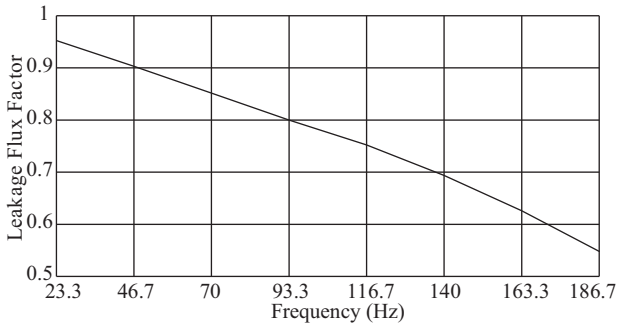

Figure 4. Leakage flux coefficient variations versus frequency variations for the designed machines.

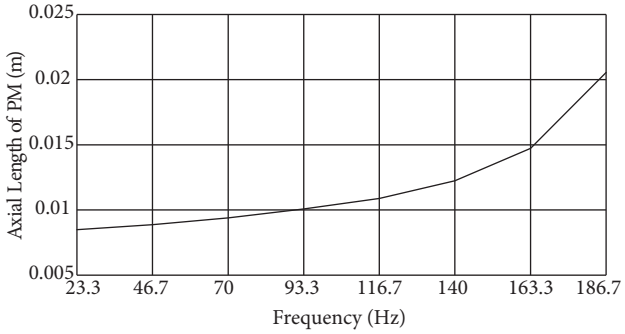

Figure 5. Permanent magnet height variations versus frequency variations for the designed machines.

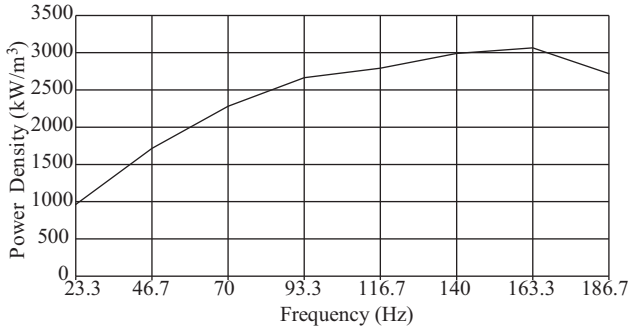

Figure 6. Power density variations versus frequency variations for the designed machines.

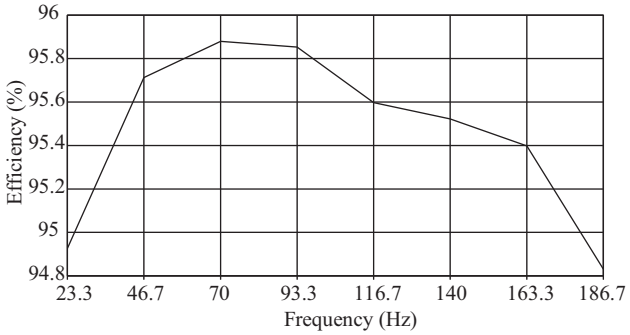

Figure 7. Efficiency variations versus frequency variations for the sample designed machines.

Table 1. Rating and main parameters of the sample machine.

Parameter	Unit	Value
Rated power	[kW]	3.7
Number of phases	-	3
Terminal voltage (rms)	[V]	111.5
Rated speed	[rpm]	1400
Air-gap length	[mm]	2
Residual flux density of PM	[T]	1.3
Coercive force of PM	[kA/m]	-955
Relative permeability of PM	-	1.021
The ratio of pole arc to pole pitch	-	0.6
Inner diameter to outer diameter ratio of stator core	-	0.516
Back EMF (rms)	[V]	111
Number of parallel paths of winding	-	1
The maximum flux density in the stator core	[T]	1.7
The maximum flux density in the rotor core	[T]	1.6

and number of pole pairs on the machine efficiency must be considered. For this purpose, four scenarios are considered as follows:

Scenario 1: The number of pole pairs, output power, and feeding voltage are considered constant. By varying the frequency in the range of 5 to 200 Hz, different machines are designed and the frequency-efficiency characteristic is determined.

Scenario 2: The frequency, output power, and feeding voltage are considered constant. By varying the number of pole pairs in the range of 1 to 20, different machines are designed and the number of pole pairs-efficiency characteristic is determined.

Scenario 3: The frequency, number of pole pairs, and feeding voltage are considered constant. By varying the output power in the range of 500 to 20,000 W, different machines are designed and the output power-efficiency characteristic is determined.

Scenario 4: The frequency, number of pole pairs, and output power are considered constant. By varying the feeding voltage in the range of 20 to 400 V, different machines are designed and the feeding voltage-efficiency characteristic is determined.

By using the proposed algorithm presented in Figure 3, these four scenarios are implemented. The results of these four scenarios are shown in Figures 8–11, respectively. In all scenarios, some constraints, such as machine stability and power capability, have been considered. Therefore, for some frequencies (or number of pole pairs or output power or voltage), it is not possible to design a machine with respect to the limitations. According to the results presented in Figures 8–11, we can consider the efficiency variations versus each of the four parameters as an exponential function. Therefore, by using the MATLAB curve fitting technique, an analytical formula is proposed to calculate the machines' efficiency in terms of frequency, number of pole pairs, output power, and feeding voltage as follows:

$$\begin{aligned} &\eta = K_1(f^{K_2})(e^{-K_3 f^{K_2}})(p^{K_4})(e^{-K_5 p^{K_4}})\times(P_{out}^{K_6})(e^{-K_7 P_{out}^{K_6}})(v^{K_8})(e^{-K_9 v^{K_8}}) \\ &K_1 = 0.6 \qquad K_2 = 0.016 \qquad K_3 = -0.046 \\ &K_4 = 0.001 \qquad K_5 = -0.037 \qquad K_6 = 0.018 \\ &K_7 = -0.049 \qquad K_8 = 0.006 \qquad K_9 = -0.05 \end{aligned} \tag{1}$$

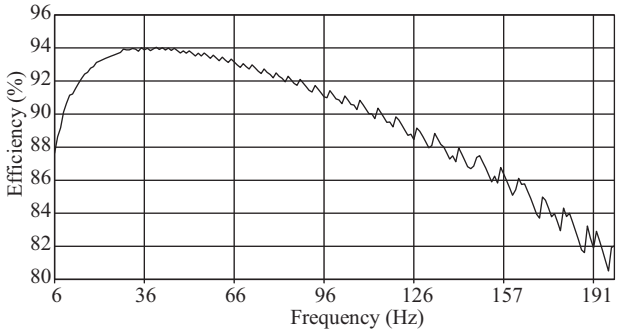

Figure 8. The efficiency versus frequency variations for the designed machines.

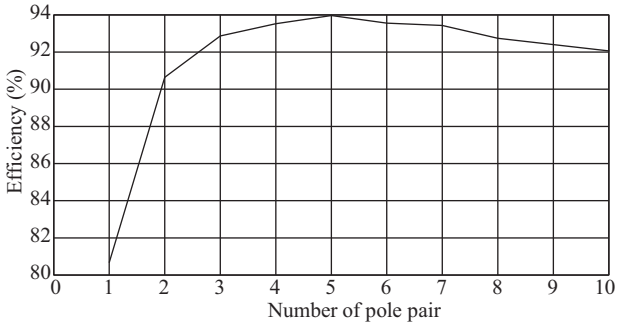

Figure 9. The efficiency versus number of pole pair variations for the designed machines.

5. Validation of the proposed formula

In order to confirm the validity of the proposed formula, several fabricated machines with different powers and speeds have been examined. These machines are illustrated in Figure 12. In the proposed algorithm, we have used the new sizing equations and relationships of the TORUS NS-AFPM machine proposed in [27]. So far,

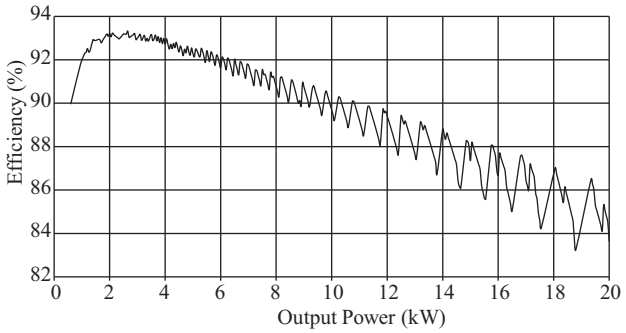

Figure 10. The efficiency versus output power variations for the designed machines.

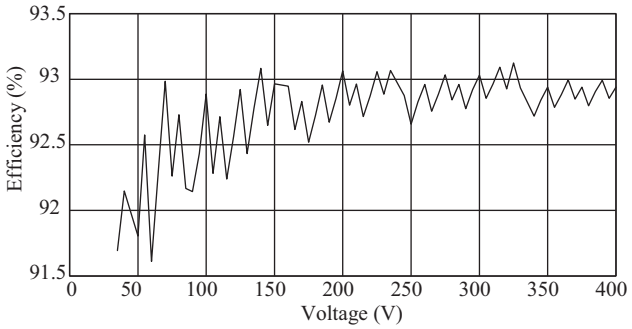

Figure 11. The efficiency versus feeding voltage variations for the designed machines.

three machines have been fabricated based on the relationships presented in this reference and we have selected them as case studies. The specifications of these machines are presented in Table 2. The performance of these machines have been evaluated in our laboratory. Here, for more clarity the performance evaluation of the 3.7 kW machine is presented. By applying a three-phase voltage with phase amplitude of 91 V and frequency of 70 Hz to the motor, the machine performances have been investigated. FEM is a precise method for validating machine performance characteristics, such as back EMF, average torque, rated power, losses. The accuracy of FEM is higher than analytical method because it considers magnetic saturation and irregular geometry [28]. Therefore, by simulating the machine in the Finite Element (FE) software, its performance characteristics have been studied. An independent-field DC generator is used as mechanical load for the motor. The specifications of this generator are given in Table 3. The terminal voltage of this generator at the motor rated speed (1400 rpm) is 186.7 V. Therefore, for a power of 3.7 kW, a current of 19.8 A amplitude flows at the terminal of the generator. The output voltage and current of the generator have been measured using a digital oscilloscope and a Hall-effect transducer. The output voltage of the generator is shown in Figure 13. In addition, the generator output current is shown in Figure 14. The voltage induced in the armature of a DC machine can be calculated as follows:

$$E_a = K\varphi\omega_m. \tag{2}$$

Where E_a, K, φ, and ω_m are induced emf voltage, constant coefficient, magnetic flux (excitation), and angular speed of the machine, respectively. The instantaneous torque of the machine is obtained as:

$$T_m = K\varphi i_a, \tag{3}$$

where T_m and i_a are instantaneous torque and armature current, respectively. By neglecting the small voltage drop on the internal resistance of the DC generator, E_a can be substituted by terminal voltage V_T. In this case, we have:

$$K\varphi = \frac{E_a}{\omega_m} \approx \frac{V_T}{\omega_m} = \frac{V_T}{(\frac{2\pi}{60}n_m)} = \frac{200}{(\frac{2\pi}{60} \times 1500)} = 1.273, \tag{4}$$

where n_m is the shaft speed in rpm. Therefore, the instantaneous speed of shaft can be calculated as follows:

$$n_m(t) = \frac{V_T(t)}{(\frac{2\pi}{60}K\varphi)} = \frac{V_T(t)}{(\frac{2\pi}{60} \times 1.273)} = 7.5V_T(t). \tag{5}$$

In addition, the instantaneous torque can be obtained as follows:

$$T_m(t) = K\varphi i_a(t) = 1.273 i_a(t). \tag{6}$$

Therefore, the instantaneous speed and torque of the machine are obtained from the instantaneous values of the terminal voltage $V_T(t)$ and the current $i_a(t)$, respectively. With respect to Eq. (5), by multiplication of Figure 13 by 7.5, the shaft speed is obtained. In addition, according to Eq. (6), by multiplication of Figure 14 by 1.273, the shaft torque is obtained. According to these figures, the average speed and torque of the machine are 1400 rpm and 25.3 N.m that are equivalent to 3.7 kW power. For more clarity, 2-D FEM has been employed to calculate the machine linear velocity and force exerting on the rotor. The machine linear velocity is shown in Figure 15. The synchronous rotational speed of the machine 1400 rpm is obtained when the linear velocity of Figure 15 multiplied by the following coefficient:

$$C_1 = \frac{60}{(\pi D_g)} = 114.5, \tag{7}$$

where D_g is the average diameter of the machine. In addition, the full-load torque 25.3 N.m is obtained through multiplying the linear force of Figure 16 by the following coefficient:

$$C_2 = \frac{D_g}{2} = 0.0834. \tag{8}$$

The machine synchronous speed is calculated as:

$$\omega_s = (\frac{2\pi}{60} \times 1400) = 146.6, \tag{9}$$

where ω_s is the synchronous speed of the machine in rad/s. The full-load torque yields the rated output power of motor 3.7 kW when multiplied by the synchronous speed. Therefore, by using the presented procedure, the output power of the machine is determined. For further validation, the machine phase current has been obtained using 2-D FEM and by measuring in the laboratory. The results of these two methods are shown in Figures 17 and 18, respectively. As is clear, the results of two methods are in good agreement with each other. In addition, by measuring machine input power P_{in} the efficiency has been calculated as follows:

$$\eta = (\frac{P_{out}}{P_{in}}) \times 100. \tag{10}$$

The performances of the two other fabricated machines have been evaluated by similar procedure. The efficiency of these three machines has been measured in the laboratory under full load condition. In addition, (1) has been used to calculate the efficiency of these machines. The results of the two methods are given in Table 4. Comparing the results shows that the error between the experimental results and proposed formula is less than 4%. Therefore, Eq. (1) has an acceptable accuracy. By using this formula at the beginning of the design process of a TORUS NS-AFPM machine, the designers can select the optimal values of frequency, number of pole pairs, and feeding voltage to yield the maximum efficiency.

6. Conclusion

In the design process of AFPM machines, the feeding voltage and frequency are usually optional parameters. Therefore, the machine designers can choose the values of these parameters arbitrarily at the beginning of the

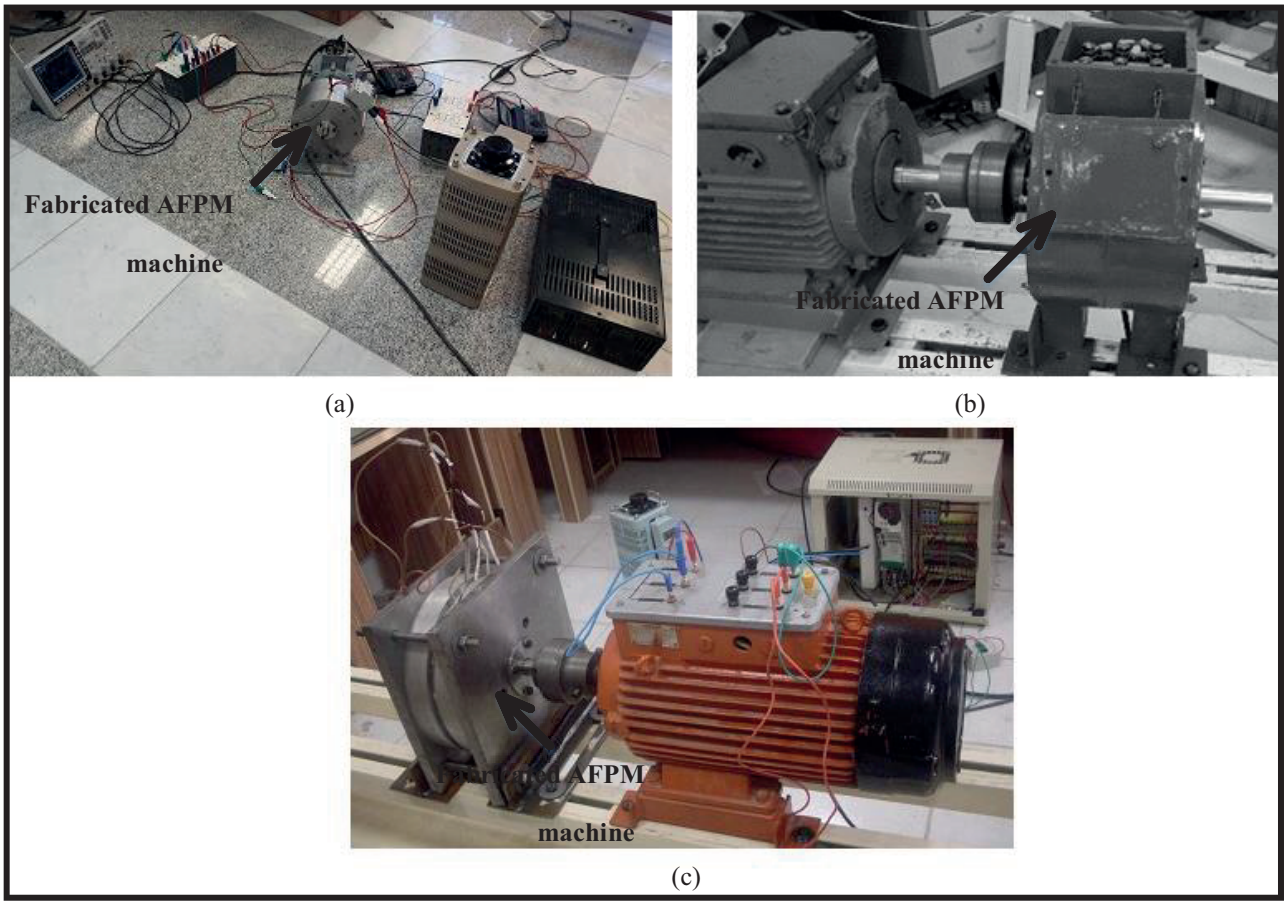

Figure 12. The fabricated TORUS NS-AFPM machines selected as case study machines (a) 0.6 kW machine, (b) 1 kW machine, and (c) 3.7 kW machine.

Table 2. Rating and main parameters of the case study machines.

Parameter	Unit	Case 1	Case 2	Case 3
Rated power	[kW]	0.6	1	3.7
Number of phases	-	3	3	3
Terminal voltage (rms)	[V]	44	33	111.5
Rated frequency	[Hz]	50	21.5	70
Number of pole pairs	[-]	2	3	3
The ratio of pole arc to pole pitch	[-]	0.6	0.6	0.6
The maximum flux density in the stator core	[T]	1.6	1.6	1.7
The maximum flux density in the rotor core	[T]	1.6	1.6	1.6

design process. In this paper, the effects of these parameters on the performance characteristics of a TORUS NS-AFPM motor have been investigated. Then a formula for calculating machine efficiency based on the frequency, number of pole pairs, machine output power, and feeding voltage has been presented. The efficiency of three fabricated TORUS NS-AFPM motor has been determined using the proposed formula and by measuring in the

Table 3. Rated specifications of the DC generator and its operating values.

Parameter	Unit	Nominal values	Operating values
Field voltage	[V]	200	200
Output voltage	[V]	200	186.7
Output current	[A]	36	19.8
Shaft speed	[rpm]	1500	1400
Shaft torque	[N.m]	45.8	25.3
Output power	[kW]	7.2	3.7

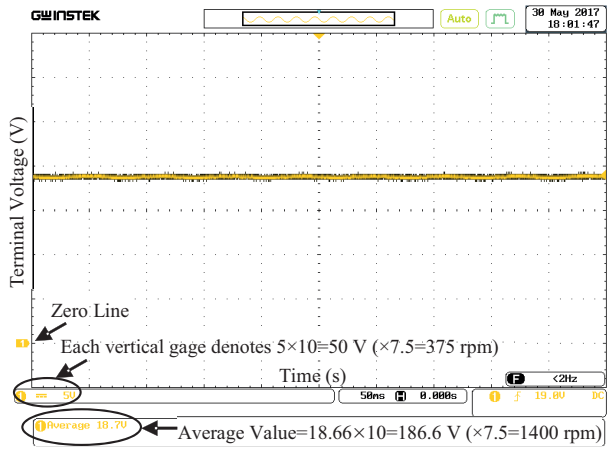

Figure 13. Experimental terminal voltage of the shaft-coupled DC generator, obtained through $a \times 10$ oscilloscope.

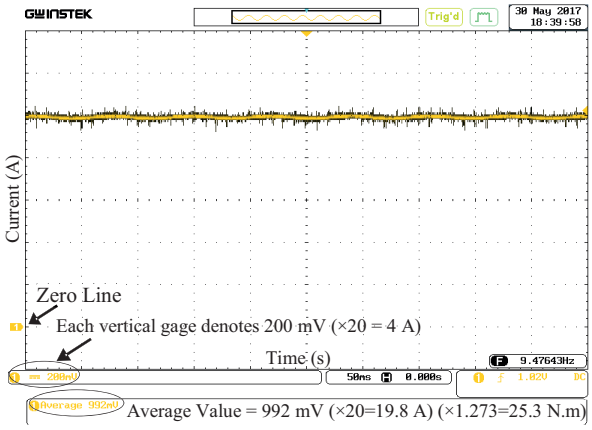

Figure 14. Experimental output current of the DC generator, obtained through a Hall-effect current transducer with attenuation 1/20 and $a \times 1$ oscilloscope probe.

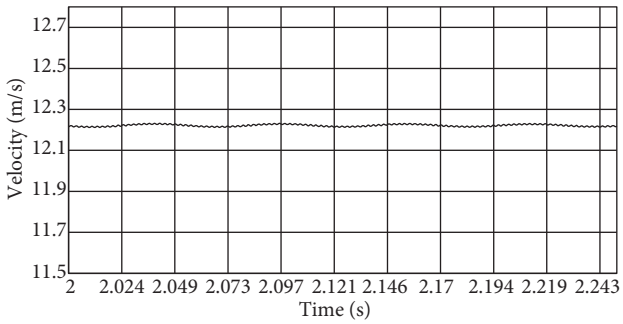

Figure 15. Linear velocity of the rotor obtained from 2-D FE simulation.

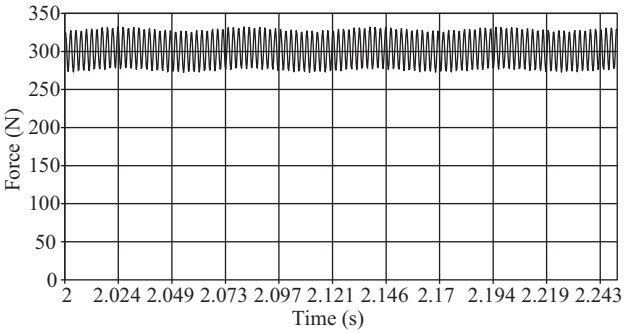

Figure 16. Linear force exerting on the rotor obtained from 2-D FE simulation.

laboratory. Comparing the results shows that the difference between the results of the two methods is less than 4%. Therefore, the TORUS NS-AFPM machine designer can use the proposed formula at the beginning of the design process to select the optimum value of the frequency, number of pole pairs, and feeding voltage regarding machine efficiency.

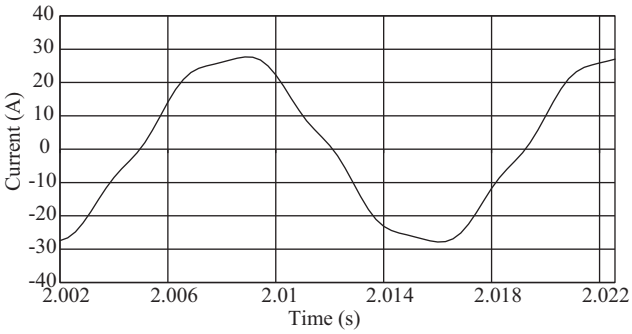

Figure 17. Armature phase current of the motor obtained by FE simulation.

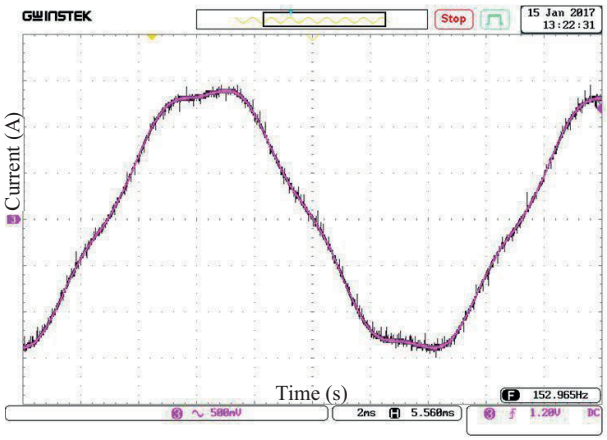

Figure 18. Armature phase current of the motor, obtained from real test.

Table 4. Efficiency of the case study machines.

Case study machines	Efficiency obtained from measurement (%)	Efficiency obtained using Eq. (1) (%)
0.6 kW machine	92	89
1 kW machine	85	88
3.7 kW machine	96.8	93

References

[1] Chan CC. Axial-field electrical machines - design and applications. IEEE Transactions on Energy Conversion 1987; EC-2 (2): 294-300. doi: 10.1109/TEC.1987.4765844

[2] Campbell P. Principles of a permanent-magnet axial-field d.c. machine. Proceedings of the Institution of Electrical Engineers 1974; 121 (12): 1489-1494. doi: 10.1049/piee.1974.0311

[3] Aydin M, Huang S, Lipo TA. Optimum design and 3D finite element analysis of nonslotted and slotted internal rotor type axial flux PM disc machines. In: IEEE 2001 Power Engineering Society Summer Meeting; Vancouver, BC, Canada; 2001. pp. 1409-1416.

[4] Aydin M, Surong H, Lipo TA. Design and 3D electromagnetic field analysis of non-slotted and slotted TORUS type axial flux surface mounted permanent magnet disc machines. In: IEEE 2001 Electric Machines and Drives Conference; Cambridge, MA, USA, USA; 2001. pp. 645-651.

[5] Nguyen TD, Tseng KJ, Zhang S, Nguyen HT. A novel axial flux permanent-magnet machine for flywheel energy storage system: design and analysis. IEEE Transactions on Industrial Electronics 2010; 58 (9): 3784-3794. doi: 10.1109/TIE.2010.2089939

[6] Lee JY, Koo DH, Moon SR, Han CK. Design of an axial flux permanent magnet generator for a portable hand crank generating system. IEEE Transactions on Magnetics 2012; 48 (11): 2977-2980. doi: 10.1109/TMAG.2012.2199093

[7] Hwang CC, Li PL, Chuang FC, Liu CT, Huang KH. Optimization for reduction of torque ripple in an axial flux permanent magnet machine. IEEE Transactions on Magnetics 2009; 45 (3): 1760-1763. doi: 10.1109/TMAG.2009.2012811

[8] Neethu S, Nikam SP, Singh S, Pal S, Wankhede AK et al. High-speed coreless axial flux permanent magnet motor with printed circuit board winding. In: IEEE 2017 Industry Applications Society Annual Meeting; Cincinnati, OH, USA; 2017. pp. 1-6.

[9] Haddad RZ, Foster SN, Strangas EG, King Y. Performance analysis of radial and axial flux fractional horsepower motors. In: IEEE 2016 Electrical Machines (ICEM) Conference; Lausanne, Switzerland; 2016. pp. 526-530.

[10] Yeşilbağ E, Ertuğrul Y, Ergene L. Axial flux PM BLDC motor design methodology and comparison with a radial flux PM BLDC motor. Turkish Journal of Electrical Engineering & Computer Sciences 2017; 25 (4): 3455-3467. doi: 10.3906/elk-1611-23

[11] Gieras JF, Wang R-J, Kamper MJ. Axial Flux Permanent Magnet Brushless Machines. New York, USA: Springer Science & Business Media, 2008.

[12] Aydin M, Huang S, Lipo T. Axial flux permanent magnet disc machines: A review. In: Conf. Record of SPEEDAM; Capri, Italy; 2004. pp. 61-71.

[13] Kahourzade S, Mahmoudi A, Gandomkar A, Rahim NA, Ping HW et al. Design optimization and analysis of AFPM synchronous machine incorporating power density, thermal analysis, and back-EMF THD. Progress In Electromagnetics Research 2013; 136: 327-367. doi: 10.2528/PIER12120204

[14] Kahourzade S, Mahmoudi A, Ping HW, Uddin MN. A comprehensive review of axial-flux permanent-magnet machines. Canadian Journal of Electrical and Computer Engineering 2014; 37 (1): 19-33. doi: 10.1109/CJECE.2014.2309322

[15] Zhao S, Liang J, Zhao Y. Optimization design and direct torque control of a flux concentrating axial flux permanent magnet motor for direct driving system. Electric Power Components and Systems 2014; 42 (14): 1517-1529. doi: 10.1080/15325008.2014.943436

[16] Zhang B, Wang Y, Doppelbauer M, Gregor M. Mechanical construction and analysis of an axial flux segmented armature torus machine. In: IEEE 2014 Electrical Machines (ICEM) Conference; Berlin, Germany; 2014. pp. 1293-1299.

[17] Aydin M, Gulec M, Demir Y, Akyuz B, Yolacan E. Design and validation of a 24-pole coreless axial flux permanent magnet motor for a solar powered vehicle. In: IEEE 2016 Electrical Machines (ICEM) Conference; Lausanne, Switzerland; 2016. pp. 1493-1498.

[18] Huang S, Aydin M, Lipo TA. Comparison of (non-slotted and slotted) surface mounted PM motors and axial flux motors for submarine ship drives. In: Third Naval Symposium on Electrical Machines; Philadelphia, USA; 2000. pp. 1-10.

[19] Huang S, Aydin M, Lipo TA. Low noise and smooth torque permanent magnet propulsion motors: Comparison of non-slotted and slotted radial and axial flux topologies. In: IEEE 2001 International Aegean Electrical Machine and Power Electronic Conference; Kuşadasi, İzmir, Turkey; 2001. pp. 1-8.

[20] Huang S, Aydin M, Lipo TA. Torque quality assessment and sizing optimization for surface mounted permanent magnet machines. In: IEEE 2001 Industry Applications Conference. Thirty-Sixth IAS Annual Meeting; Chicago, IL, USA, USA; 2001. pp. 1603-1610.

[21] Neethu S, Pal S, Wankhede AK, Fernandes BG. High performance axial flux permanent magnet synchronous motor for high speed applications. In: IEEE 2017 Industrial Electronics Society (IECON); Beijing, China; 2017. pp. 5093-5098.

[22] Lim DK, Cho YS, Ro JS, Jung SY, Jung HK. Optimal design of an axial flux permanent magnet synchronous motor for the electric bicycle. IEEE Transactions on Magnetics 2016; 52 (3): 1-4. doi: 10.1109/TMAG.2015.2497374

[23] Huang S, Luo J, Leonardi F, Lipo TA. A Comparison of power density for axial flux machines based on general purpose sizing equations. IEEE Power Engineering Review 1997; 17 (11): 55.

[24] Mahmoudi A, Ping HW, Rahim NA. A comparison between the TORUS and AFIR axial-flux permanent-magnet machine using finite element analysis. In: IEEE 2011 Electric Machines & Drives Conference (IEMDC); Niagara Falls, ON, Canada; 2011. pp. 242-247.

[25] Baghayipour M, Darabi A, Dastfan A. An analytical model of harmonic content no-load magnetic fields and Back EMF in axial flux PM machines regarding the iron saturation and winding distribution. COMPEL-The International

Journal for Computation and Mathematics in Electrical and Electronic Engineering 2018; 37 (1): 54-76. doi: 10.1108/COMPEL-01-2017-0003

[26] Park HJ, Jung HK, Jung SY, Chae YH, Woo DK. Field reconstruction method in axial flux permanent magnet motor with overhang structure. IEEE Transactions on Magnetics 2017; 53 (6): 1-4. doi: 10.1109/TMAG.2017.2653839

[27] Darabi A, Baghayipour M, Mirzahosseini R. An extended analytical algorithm for optimal designing of a TORUS-type non-slotted axial-flux permanent magnet motor. Journal of Control, Automation and Electrical Systems 2017; 28 (6): 748-761. doi: 10.1007/s40313-017-0337-8

[28] Reza MM, Ahmad A, Kumar P, Srivastava RK. Semi-analytical model for triangular skewed permanent magnet axial flux machine. In: IEEE 2017 Transportation Electrification Conference (ITEC-India); Pune, India; 2017. pp. 1-5.